Comparative Raman spectroscopy of individual and bundled double wall carbon nanotubes

Pascal Puech, Sébastien Nanot, Bertrand Raquet, Jean-Marc Broto, Marius Millot, Abdul Waheed Anwar, Emmanuel Flahaut, Wolfgang Bacsa

▶ **To cite this version:**

Pascal Puech, Sébastien Nanot, Bertrand Raquet, Jean-Marc Broto, Marius Millot, et al.. Comparative Raman spectroscopy of individual and bundled double wall carbon nanotubes. physica status solidi (b), 2010, 248 (4), pp.974-979. 10.1002/pssb.200945548 . hal-03474402

HAL Id: hal-03474402
https://hal.science/hal-03474402

Submitted on 10 Dec 2021

HAL is a multi-disciplinary open access archive for the deposit and dissemination of scientific research documents, whether they are published or not. The documents may come from teaching and research institutions in France or abroad, or from public or private research centers.

L'archive ouverte pluridisciplinaire **HAL**, est destinée au dépôt et à la diffusion de documents scientifiques de niveau recherche, publiés ou non, émanant des établissements d'enseignement et de recherche français ou étrangers, des laboratoires publics ou privés.

Open Archive Toulouse Archive Ouverte (OATAO)
OATAO is an open access repository that collects the work of Toulouse researchers and makes it freely available over the web where possible.

This is an author-deposited version published in: http://oatao.univ-toulouse.fr/
Eprints ID: 5716

To link to this article: DOI: 10.1002/pssb.200945548
URL : http://dx.doi.org/10.1002/pssb.200945548

To cite this version:

Puech, Pascal and Nanot, Sébastien and Raquet, Bertrand and Broto, Jean-Marc and Millot, Marius and Anwar, Abdul Waheed and Flahaut, Emmanuel and Bacsa, Wolfgang *Comparative Raman spectroscopy of individual and bundled double wall carbon nanotubes.* (2010) physica status solidi b, vol. 248 (n° 4). pp. 974-979. ISSN 0370-1972

Any correspondence concerning this service should be sent to the repository administrator: staff-oatao@listes.diff.inp-toulouse.fr

DOI 10.1002/pssb.200945548

Comparative Raman spectroscopy of individual and bundled double wall carbon nanotubes

Pascal Puech[1], Sébastien Nanot[2], Bertrand Raquet[2], Jean-Marc Broto[2], Marius Millot[2], Abdul Waheed Anwar[1], Emmanuel Flahaut[3], and Wolfgang Bacsa[*,1]

[1] Université de Toulouse, UPS, CNRS, CEMES, 29 rue Jeanne Marvig, 31055 Toulouse, France
[2] Université de Toulouse, UPS-INSA, CNRS, LNCMI, 143 avenue de Rangueil, 31077 Toulouse, France
[3] Université de Toulouse, UPS, CNRS, Institut Carnot, CIRIMAT, 31062 Toulouse, France

Keywords carbon, nanotubes, Raman spectra, phonons

[*] Corresponding author: e-mail wolfgang.bacsa@cemes.fr, Phone: +33 5 6225 7822, Fax: +33 5 6225 7999

Abstract

Raman spectra of individual double wall carbon nanotubes(DWs) on silica show a splitting of the G band due to contributions of the inner and outer tube when using a excitation energy in resonance with the inner metallic tube and outer semiconducting tube. The spectral splitting indicates strong coupling while a previous report [Nanoletters **8**, 3879 (2008)] shows uncoupled inner and outer tubes. The spectral line widths are comparable to what has been observed for individual single wall carbon nanotubes (SWs) or graphene. The spectral position of the inner tube is consistent with previous extrapolations from measurements under high pressure and on chemically doped double wall tubes. Bundling of DWs leads to heterogeneous increase of the G band line width. Increased laser power shifts the G band of the outer tube to higher energies and modifies its line shape.

Double wall carbon nanotubes (DWs) are an attractive alternative to single wall carbon nanotubes (SWs) [1]. The internal tube with diameter comparable to SWs, is embedded in the outer tube making it less susceptible to interactions with its environment which influences its electronic states. The outer tube in DWs interacts with the substrate and its coupling with the environment depends on whether the outer tube is semiconducting or metallic. DWs can be grown either by conversion of peapods [2] or through the catalytic chemical vapour deposition method (CCVD) [3]. In the case of DWs grown with the CCVD method, the inner and outer tubes are formed at the same time while in the case of peapod conversion, the inner tube is formed in the presence of an already present outer tube.

There exists clear differences between Raman bands of SWs, DWs and multi-wall carbon nanotubes (MWs). For SWs, the disorder induced D band and the second order G'_{2D} bands have one main band. For DWs or MWs, the D and G'_{2D} band consists of several components or bands with shoulders.

For SWs, the G^+ mode have a half width at half maximum (HWHM) of $3\,cm^{-1}$ which is lower than in graphite ($7\,cm^{-1}$) [4]. For DWs, the G band is broad and it was first assumed to be simply the sum of SW contributions. Chemical doping and high pressure experiments by Chen et al. [5] and Puech et al. [7, 6] have shown that the G band is composed of at least two separated bands attributed to the inner and outer tubes. The frequency of the inner tube is at $1581\,cm^{-1}$ and the frequency of the outer tube is higher and close to $1592\,cm^{-1}$. The frequency of the inner tubes has been found as expected to be less sensitive to external perturbations than the frequency of the outer tube [8]. An additional less intense electronic interlayer contribution which could be fitted by a single lorentzian band has been observed at lower frequency ($1560\,cm^{-1}$). All the G band contributions together are forming a broad band for bundled

DWs. The interpretation of DWs based on SWs is inconsistent. The wall interaction has to be taken into account as evidenced by findings on doped DWs and the influence of high pressure on DWs. The coupling of the wall is essential for DW and MW Raman bands.

The radial breathing modes (RBMs) are due to collective radial displacement of the atoms. RBMs can be very intense within a narrow spectral range, corresponding to van Hove singularities in the joined density of states. This has been used to determine the transition energy for both metallic and semi-conducting SWs versus the tube diameter [9, 10] and has been compared to photoluminescence excitation spectroscopy measurements giving also access to the electronic transition energies for semiconducting tubes. [11, 12] The resonance profile for the RBM of individual tubes is particularly narrow (80 meV) [10]. The tube diameter can be extracted using the RBM frequency and by combining with the energy transition, one can determine the tube chirality [13]. However, the exact spectroscopic location of the resonance is influenced by the interaction of the tube with its environment and can shift by up to 100 meV [9, 10].

For DWs, the interaction between the tubes can modify the RBMs frequencies [14, 15]. Comparing DWs grown by CCVD and obtained from peapod conversion one finds also differences in the G band lineshape. The pressure transmission on the inner tube is delaying for DWs from peapods as compared for DWs grown with the CCVD method when increasing the pressure [6]. The two types of DWs show also differences in the G'_{2D} band. The G'_{2D} band for DWs grown form peapods has two separated contributions due to inner and outer tubes while the G'_{2D} band for DWs grown with the CCVD method shows a single band with a shoulder similar to what is observed for graphite. For a DWs to be electrically conducting only one of the tubes needs to be metallic.

A recent Raman study [16] of individual DWs shows spectra for different metallic and semi-conducting tube configurations for inner and outer tubes. Using S for semiconducting and M for metallic tubes, we can use the following notation for the four combinations of tubes for DWs: M@M, S@M, M@S, S@S (inner@outer). The frequency of the RBMs and excitation energy provide the opportunity to determine the tube structure (n,m).

In this paper, we report Raman spectra from an individual DW excited at three different excitation wavelengths (468–568 nm). We compare our findings with bundles of DWs. The spectral position and HWHM are discussed and we investigate the influence of laser power on the spectra.

DWs were prepared by the CCVD method as described in Ref. [3]. High-resolution electron microscopy shows that the inner tubes of the DW association have a diameter ranging from 0.6 to 2.3 nm. The DWs have been dispersed using a 1,2-dichloroethane (DCE) solution and deposited on an oxidized silicon substrate pre-patterned with secondary Au electrodes.

The DCE solution with the DW has been sonicated for a short time (less than 10 min) and low power (less than 35 W). This debundles the DW to some degree. Only the top portion of the solution has been used containing isolated DWNTs. The samples have been rinsed with acetone and ethanol after deposition to remove the DCE. From comparative transport measurements we conclude that the tubes have not been damaged by the sonication process.

Individual tubes (typical length: 3 μm) are localized by scanning force microscopy. The tubes have been at a later stage connected with Pd electrodes using e-beam lithography and lift-off technique with a distance of 0.5 μm between the electrodes. We can discriminate tubes which are bundled and individual tubes using scanning force microscopy. From the scanning force microscopy images we can estimate the tube height (1.4 ± 0.4 nm for the individual DW discussed here). Height variation of the substrate results in a relative large uncertainty in the tube height. Preliminary gate-voltage dependent conductance measurements performed under ambient conditions show that the investigated tube is conducting.

Raman spectra were acquired on a T64000 spectrometer from Horiba Jobin-Yvon industry. The laser power was measured after the objective. Polarization has been selected along the tube axis according to the scanning force microscopy images of the tube to have the maximum light absorption [17].

We find that laser heating is less important for individual DWs in contact with the substrate or connected to the metal electrode. We use 1 mW with an objective of magnitude 100. Bundles of DWs are more sensitive to laser power. To reduce heating effects on DW bundles we use a low laser power, typically 0.1 mW and an objective of magnitude 40 to increase the focal spot size (2 μm) decreasing the power density. All spectra have been recorded by integrating the signal from the scattered light for 100–500 s. For the power dependent measurements, we increased the laser power up to 3 mW.

Figure 1 shows the Raman G band region of the individual DW and bundled DWs excited at three different excitation wavelengths. The spectra from the individual DW

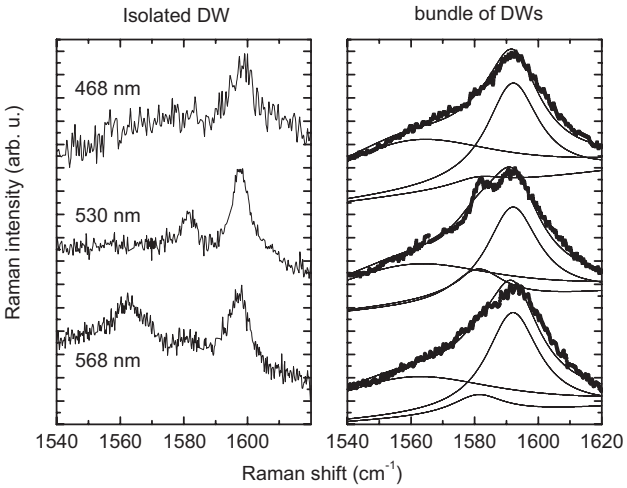

Figure 1 G band of individual DW (left side) and bundles of DWs (right side) using three different excitation energies.

Table 1 G band and band due to interlayer coupling for bundled and individual DWs.

		in bundle (647 nm)	individual
interlayer coupling	HWHM (cm^{-1})	35	8
	ω (cm^{-1})	1560	1563
G band inner tube	HWHM (cm^{-1})	10	4
	ω (cm^{-1})	1581	1580
G band outer tube	HWHM (cm^{-1})	10	4
	ω (cm^{-1})	1592	1597

are narrower and contain up to three spectral bands. Bundles of DWs show a larger and asymmetric G band. The spectra of the DW bundles have been fitted by three Lorentzian line shapes using fixed spectral position and taking the relative intensities as a free parameter [6]. The fitted G band positions are reported in Table 1. The HWHM is much smaller for individual DWs. The HWHM of the G band of the inner and outer tube is $4 \pm 1\,cm^{-1}$ which is the same HWHM observed for individual SWs or for single layer graphene [18]. The HWHM depends on the decay process [19] and is increased by the number of defects. It has been shown that for SWs that the HWHM varies with applied voltage, with a minimum value at $4\,cm^{-1}$ [20, 21]. For bundles of DWs the HWHM is $10\,cm^{-1}$. This larger HWHM for bundles can be explained by the interaction with neighbouring tubes leading to heterogeneous line broadening. For comparison, pyrolytic graphite has a similar HWHM ($7\,cm^{-1}$) [22]. Few reports investigate the number of tubes in the bundle. Jiang et al. [23] show that the Fano line which is weak for an individual tube in air and without electrode contact, is strongly enhanced in a bundle and they observe no change of HWHM. Nguyen et al. [24] shows that in air, oxygen doping of individual metallic tube move the Fermi level leading to the disappearance of the Fano line but by controlling the gate voltage, the Fano line shape can be restored. In bundles the atoms in contact with air, are reduced and this prevents doping and consequently the Fermi level is positioned close to the K point. The increase of the broadening for DWs can be connected to the number of DWs in each bundle and the fact that several bundles are observed at the same time. A variation in doping (Fermi level position) of each bundles due to oxygen leads to a change in frequency and resulting in a broader band when observing several bundles at the same time. For both metallic [24] and semiconducting [25] tubes, this effect is observed. We consequently conclude that heterogeneity and not defects is at the origin of the increase of the measured HWHM.

For the spectra from an individual DW (Fig. 1), the spectral position of the G band of the inner tube is at $1580 \pm 2\,cm^{-1}$ and for the outer tube at $1597 \pm 2\,cm^{-1}$. The spectral position of the inner tube is consistent with the extrapolated spectral position deduced from high pressure experiments [7] and when studying the influence by chemical doping of DWs [5]. The spectral position of the G band for the outer tube is relatively high. When changing the excitation energy, we can see considerable changes in the intensity of the inner tube which we can attribute to changes in the resonance condition. At 568 nm an additional band is observed at $1563\,cm^{-1}$ which has been previously observed and identified as being associated with electronic coupling with the environment and the outer tube [6]. Nguyen et al. have shown that SWs exposed to air leads to strong p-doping of the SWs [24]. The high frequency associated to the outer tube is consistent with this explanation.

To identify the tube structure we use the electronic transition energies from the Kataura plot [26] with the following expression as reported by Araujo et al. [12]:

$$E_{ii}(p, d_t) = \frac{\beta_p \cos(3\theta)}{d_t^2} + a\,\frac{p}{d_t}\left[1 + b\log\left(\frac{c}{p/d_t}\right)\right] + \frac{\gamma_p}{d_t},$$

where p is the transition index ranging from 1 to 6, d_t the tube diameter, θ the chiral angle, a, b, c constant values, β_p a correction due to the chirality for upper and lower branches and γ_p a correction associated to exciton localization.

Using this analytical expression and $\gamma_p = 0$, one can estimate accurately the transition energies for E_{11}^S, E_{22}^S and E_{11}^M. For the E_{33}^S and E_{44}^S or E_{55}^S and E_{66}^S, we use $\gamma = 0.305$ for unbound excitonic states as suggested by the authors. For the E_{22}^M transition, we use $\gamma = 0.305$ which fits well with the experimental results of Sfeir et al. [27] reducing the uncertainty to less than 0.1 eV for the corresponding transition energies.

From the possible diameters considering only resonant Raman scattering experiment, using the Fig. 2, we can find several configurations with increasing diameter: S@S corresponding roughly to an inner diameter of 0.6 nm, M@S corresponding roughly to an inner diameter of 1 nm and S@M corresponding roughly to an inner diameter of 1.7 nm. When using height estimation from scanning force microscopy, we conclude that the M@S configuration with

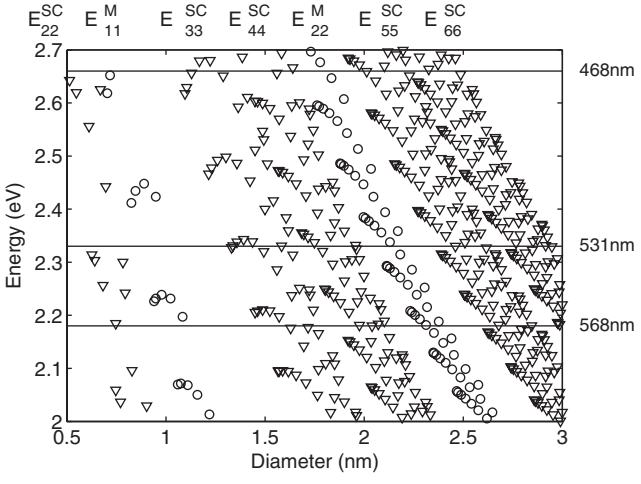

Figure 2 Optical transition energies from Araujo et al. [12]. The circles show the transition energies for metallic and the triangles show the transition energies for semiconducting tubes.

an inner diameter of 1 nm and an outer one of 1.7 nm is the most likely configuration for the DW investigated here. This configuration agrees with our preliminary electronic transport measurements which show a small on/off ratio in the source-drain current *versus* gate voltage dependence characteristic for metallic tubes [28]. From the gate voltage at the largest variation of the source drain current we find that the semiconducting tube is p doped.

We note that for a similar DW, M@S configuration and similar diameter, Villalpando-Paez et al. [16] found a G band frequency of 1591 cm^{-1} without separating between contributions from the inner and the outer tube although the tube diameters are similar and the DWs have been grown using the CCVD method. Interestingly no splitting is observed here for the G'_{2D} band while Villalpando-Paez et al. [16] observe a clear splitting of the G'_{2D} as in the case for DWs grown from the peapod method. This shows that the two types of behaviour of DWs, either strongly coupled or decoupled can be observed for CCVD grown tubes. This can be explained by the different growth parameters used in the CCVD method which apparently play an important role in the inter wall spacing. In our case, the inner and outer tube are strongly coupled, leading to a clear difference in the spectral positions.

Figure 3 shows the RBM region and the second order D band (G'_{2D} band) of the individual DW and bundled DWs using 531 nm excitation. The absence of intense RBM bands in the case of individual tube indicates that the excitation does not exactly coincide with the resonance maximum with neither of the two tubes. Nevertheless, for the individual DW we observe an RBM band at 250 cm^{-1} consistent with an inner tube of 0.94 nm diameter. In the range 200–300 cm^{-1}, this is the only feature. In the range 100–200 cm^{-1}, several bands are observed. A less intense spectral band at 150 cm^{-1} consistent with the RBM of a outer tube of 1.61 nm diameter can be associated to a DW. We use the constants determined by Telg et al. [9] for the determination of the diameter from the RBM frequency. From the Kataura plot reported in Fig. 2, we found an chirality of (12,0) for the inner tube and a chirality of (20,1) for the outer tube. The wall spacing is 0.34 nm consistent with the interlayer spacing in graphite. For the attribution so far, we have assumed that the coupling between the walls does not affect the RBMs frequency. The (12,0)@(20,1) tube combination is the most likely. We note that Kuzmany et al. [14] have reported that the inner tube frequency is dependent to the wall spacing leading to a small correction. For bundles we observe several RBM's in the 140–180 cm^{-1} and 240–270 cm^{-1} spectral range. We find that the G'_{2D} band for isolated tubes is less broad then for DW bundles.

Conductance measurements, Raman spectra in the RBMs range and AFM measurements are consistant with an M@S configuration. An outer diameter of 1.61 nm and an inner diameter of 0.94 nm can be deduced when assigning the tubes to the (12,0)@(20,1) configuration.

By varying the laser power from 1 to 3 mW for the individual DW on SiO_2 using 568 nm excitation, we observe changes in the G band of the outer tube and the disappearance of the additional spectral band at 1563 cm^{-1} (Fig. 4). The fitted band positions are reported in Table 2. It has been

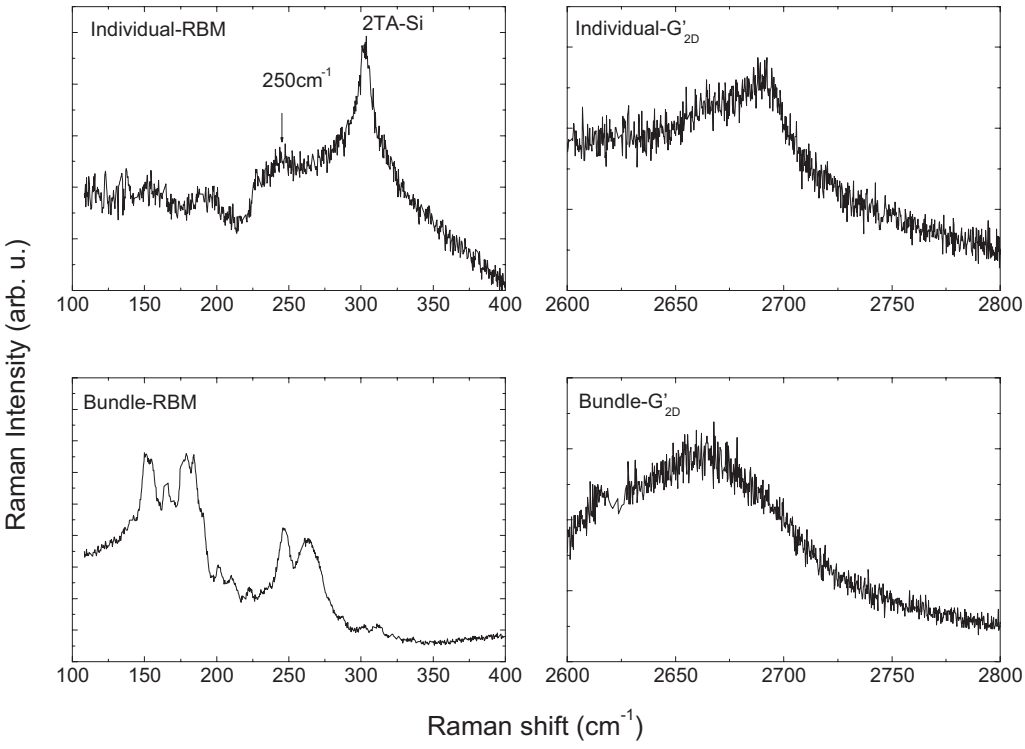

Figure 3 Frequency range of RBM and G'_{2D} band of individual DW on SiO_2 (top) and DW bundles (below) at 531 nm.

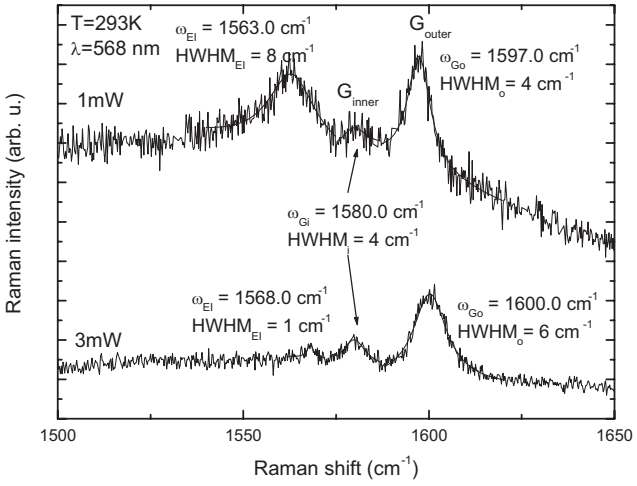

Figure 4 Raman G band of individual DW excited at two different laser powers.

Table 2 G band position for individual DW for two laser powers excited at 568 nm.

		1 mW	3 mW
interlayer coupling	HWHM (cm^{-1})	8	1 (very weak)
	ω (cm^{-1})	1563	1568 (very weak)
inner tube	HWHM (cm^{-1})	4	4
	ω (cm^{-1})	1580	1580
outer tube	HWHM (cm^{-1})	4	6
	ω (cm^{-1})	1597	1600

previously found that this additional band is correlated to the G band shift of the outer tube with chemical doping [6]. The G band of the outer tube shifts to higher frequency and broadens with laser power while the G band of the inner tube remains at the same spectral position. A temperature increase, however, is known to shift the G band to lower frequency and broadening the band uniformly. The up-shift and non-uniform broadening can be associated to doping. Doping can be due to substrate and/or oxygen exposure. Doping can lead to an upshift of the G band and can increase the HWHM for semi-conducting tubes [25]. This is compatible with assuming a outer semiconducting tube for our observation of an individual tube.

Electrical conductance measurements have shown that the G band associated to the outer tube can up shift or down shift and shows hysteresis when scanning the applied voltage [8]. When the tube lies on an insulating SiO_2 layer, the Fermi level of the outer tube can be influenced when illuminated through its interaction with its environment (oxygen and substrate). The more or less disappearance of the additional band observed at 1563 cm^{-1} attributed to electronic coupling [6], is consistent with a change in the Fermi level position. A less intense band remains at 1568 cm^{-1} and the background is strongly reduced. We note that far from the *K* point, electronic interlayer coupling is removed [24]. In the present case, the G band frequency of the inner tube is not influenced by the laser power. The G band position (1580 cm^{-1}) shows that the interaction with the outer tube is still present and absence of a power induced frequency shift is consistent with no large charge transfer to the inner tube as has been reported by Chen et al. [5].

Consistent with what has been reported by Nguyen et al. [24], the integrated intensity of all bands of the G band is conserved when normalized to the D band intensity. In our case, the inner tube can be used as a reference. The integrated intensity of the G band associated to the outer tube compared to the intensity of the G band associated to the inner tube is increased by 40% when the laser power increases from 1 to 3 mW. At the same time, the huge background is reduced as does the band associated with electronic interlayer coupling. This shows that there is an intensity transfer from the electronic interlayer signal to the G band of the outer tube.

In summary, we find that coupled individual DWs show narrow and separated G bands corresponding to the inner and outer tube. The line-widths of the G band of the inner and outer tube are comparable to what has been reported for individual SWs and single layer graphene. Bundling broadens the G band considerably. Using height estimation from scanning force microscopy, excitation wavelength and preliminary transport measurements, we can identify the tube configuration to be M@S. An increase of the laser power at 568 nm leads to a preferential modification of the outer tube and is correlated with the disappearance of a band associated to electronic interlayer coupling.

References

[1] R. Pfeiffer, T. Pichler, Y. A. Kim, and H. Kuzmany, Double wall carbon nanotubes, in: Carbon Nanotubes, Advanced Topics in the Synthesis, Structure, Properties and Applications, edited by A. Jorio, G. Dresselhaus, and M. S. Dresselhaus (Springer, Heidelberg, 2008), p. 495.

[2] S. Bandow, M. Takizawa, K. Hirahara, M. Yudasaka, and S. Iijima, Chem. Phys. Lett. **337**, 48 (2001).

[3] E. Flahaut, R. Bacsa, A. Peigney, and Ch. Laurent, Chem. Commun. **12**, 1442 (2003).

[4] A. Jorio, C. Fantini, M. S. S. Dantas, M. A. Pimenta, A. G. Souza Filho, Ge. G. Samsonidze, V. W. Brar, G. Dresselhaus, M. S. Dresselhaus, A. K. Swan, M. S. Ünlü, B. B. Goldberg, and R. Saito, Phys. Rev. B **66**, 115411 (2002).

[5] G. Chen, S. Bandow, E. R. Margine, C. Nisoli, A. N. Kolmogorov, V. H. Crespi, R. Gupta, G. U. Sumanasekera, S. Iijima, and P. C. Eklund, Phys. Rev. Lett. **90**, 257403 (2003).

[6] P. Puech, A. Ghandour, A. Sapelkin, C. Tinguely, E. Flahaut, D. J. Dunstan, and W. Bacsa, Phys. Rev. B **78**, 045413 (2008).

[7] P. Puech, H. Hubel, D. Dunstan, R. R. Bacsa, C. Laurent, and W. S. Bacsa, Phys. Rev. Lett. **93**, 095506 (2004).

[8] S. Yuan, Q. Zhang, Y. You, Z. X. Shen, D. Shimamoto, and M. Endo, Nano Lett. **9**, 383 (2009).

[9] H. Telg, J. Maultzsch, S. Reich, F. Hennrich, and C. Thomsen, Phys. Rev. Lett. **93**, 177401 (2004).

[10] C. Fantini, A. Jorio, M. Souza, M. S. Strano, M. S. Dresselhaus, and M. A. Pimenta, Phys. Rev. Lett. **93**, 147406 (2004).
[11] S. M. Bachilo, M. S. Strano, C. Kittrell, R. H. Hauge, R. E. Smalley, and R. B. Weisman, Science **298**, 2361 (2002).
[12] P. T. Araujo, S. K. Doorn, S. Kilina, S. Tretiak, E. Einarsson, S. Maruyama, H. Chacham, M. A. Pimenta, and A. Jorio, Phys. Rev. Lett. **98**, 067401 (2007).
[13] A. M. Rao, E. Richter, S. Bandow, B. Chase, P. C. Eklund, K. A. Williams, S. Fang, K. R. Subbaswamy, M. Menon, A. Thess, R. E. Smalley, G. Dresselhaus, and M. S. Dresselhaus, Science **275**, 187 (1997).
[14] R. Pfeiffer, F. Simon, H. Kuzmany, and V. N. Popov, Phys. Rev. B **72**, 161404 (2005).
[15] R. R. Bacsa, A. Peigney, Ch. Laurent, P. Puech, and W. S. Bacsa, Phys. Rev. B **65**, 161404 (2002).
[16] F. Villalpando-Paez, H. Son, D. Nezich, Y. P. Hsieh, J. Kong, Y. A. Kim, D. Shimamoto, H. Muramatsu, T. Hayashi, M. Endo, M. Terrones, and M. S. Dresselhaus, Nanoletters **8**, 3879 (2008).
[17] H. Ajiki and T. Ando, Jpn. J. Appl. Phys. Suppl. **43-1**, 107 (1994).
[18] A. Das, S. Pisana, B. Chakraborty, S. Piscanec, S. K. Saha, U. V. Waghmare, K. S. Novoselov, H. R. Krishnamurthy, A. K. Geim, A. C. Ferrari, and A. K. Sood, Nature Nanotechnol. **3**, 210 (2008).
[19] G. P. Srivastava, The Physics of Phonons (Adam Hilger, Bristol, 1990).
[20] J. C. Tsang, M. Freitag, V. Perebeinos, J. Liu, and Ph. Avouris, Nature Nanotechnol. **2**, 725 (2007).
[21] A. Jorio, C. Fantini, M. S. S. Dantas, M. A. Pimenta, A. G. Souza Filho, Ge. G. Samsonidze, V. W. Brar, G. Dresselhaus, M. S. Dresselhaus, A. K. Swan, M. S. Unlu, B. B. Goldberg, and R. Saito, Phys. Rev. B **66**, 115411 (2002).
[22] M. Hanfland, H. Beister, and K. Syassen, Phys. Rev. B **39**, 12598 (1989).
[23] C. Jiang, K. Kempa, J. Zhao, U. Schlecht, U. Kolb, T. Basché, M. Burghard, and A. Mews, Phys. Rev. B **66**, 161404(R) (2002).
[24] K. T. Nguyen, A. Gaur, and M. Shim, Phys. Rev. Lett. **98**, 145504 (2007).
[25] A. Das and A. K. Sood, Phys. Rev. B **79**, 235429 (2009).
[26] H. Kataura, Y. Kumazawa, Y. Maniwa, I. Umezu, S. Suzuki, Y. Ohtsuka, and Y. Achiba, Synth. Met. **103**, 2555 (1999).
[27] M. Y. Sfeir, T. Beetz, F. Wang, L. Huang, X. M. Henry Huang, M. Huang, J. Hone, S. O'Brien, J. A. Msewich, T. F. Heinz, L. Wu, Y. Zhu, and L. E. Brus, Science **312**, 554 (2006).
[28] S. Wang, X. L. Liang, Q. Chen, Z. Y. Zhang, and L.-M. Peng, J. Phys. Chem. B **109**, 17361 (2005).